Title

The Antioxidant/Nitric Oxide-Quenching Agent Cobinamide Prevents Aortic Disease in a Mouse Model of Marfan Syndrome

Journal

JACC Basic to Translational Science, 9(1)

ISSN

2452-302X

Authors

Kalyanaraman, Hema

Casteel, Darren E

Cabriales, Justin A

et al.

Publication Date

2024

DOI

10.1016/j.jacbts.2023.07.014

Peer reviewed

JACC: BASIC TO TRANSLATIONAL SCIENCE VOL. 9, NO. 1, 2024

ORIGINAL RESEARCH - PRECLINICAL

The Antioxidant/Nitric Oxide-Quenching Agent Cobinamide Prevents Aortic Disease in a Mouse Model of Marfan Syndrome

Hema Kalyanaraman, PhD,[a,*] Darren E. Casteel, PhD,[a,*] Justin A. Cabriales, BS,[a] John Tat, PhD,[a] Shunhui Zhuang, MD,[a] Adriano Chan, BS,[a] Kenneth L. Dretchen, PhD,[b] Gerry R. Boss, MD,[a] Renate B. Pilz, MD[a]

VISUAL ABSTRACT

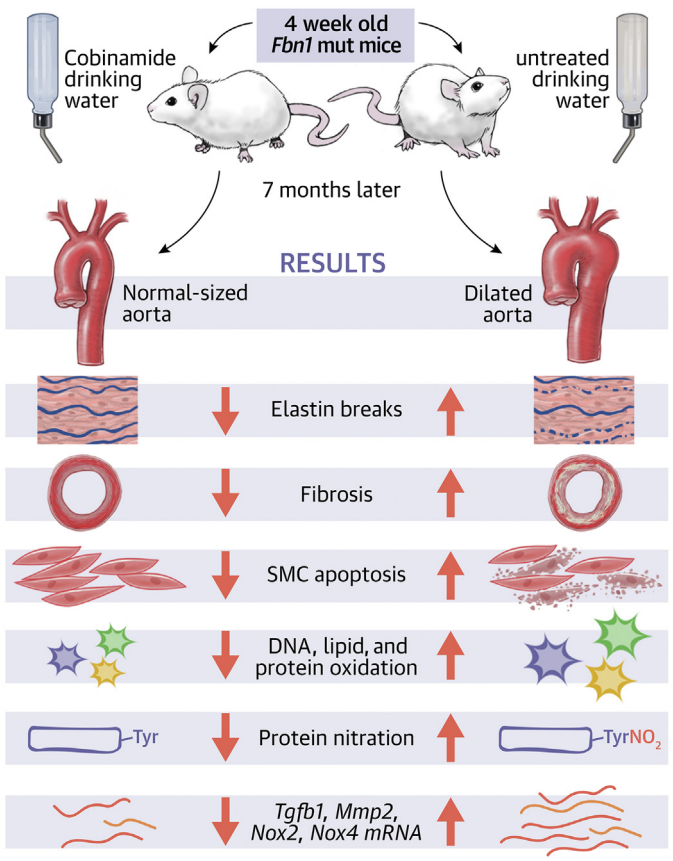

Kalyanaraman H, et al. J Am Coll Cardiol Basic Trans Science. 2024;9(1):46-62.

HIGHLIGHTS

- **MFS is a frequent cause of familial thoracic aortic aneurysms, and mortality from aortic rupture remains high, despite current treatments with β-adrenergic and angiotensin receptor blockers.**
- **Based on recent evidence implicating oxidative stress and excess NO signaling in the aortic pathology of MFS, we studied the novel antioxidant and NO-quenching agent cobinamide in a MFS mouse model.**
- **Cobinamide normalized markers of oxidative and nitrosative stress, prevented characteristic pathologic changes in the aorta, and reduced aortic dilation.**
- **Cobinamide had favorable safety and pharmacokinetic profiles, suggesting it could be a novel disease-modifying treatment for MFS.**

From the [a]Department of Medicine, University of California-San Diego, La Jolla, California, USA; and the [b]Mesa Science Associates, Frederick, Maryland, USA. *Drs Kalyanaraman and Casteel contributed equally to this work and are joint first authors.

ISSN 2452-302X https://doi.org/10.1016/j.jacbts.2023.07.014

ABSTRACT

Major pathologic changes in the proximal aorta underlie the life-threatening aortic aneurysms and dissections in Marfan Syndrome; current treatments delay aneurysm development without addressing the primary pathology. Because excess oxidative stress and nitric oxide/protein kinase G signaling likely contribute to the aortopathy, we hypothesized that cobinamide, a strong antioxidant that can attenuate nitric oxide signaling, could be uniquely suited to prevent aortic disease. In a well-characterized mouse model of Marfan Syndrome, cobinamide dramatically reduced elastin breaks, prevented excess collagen deposition and smooth muscle cell apoptosis, and blocked DNA, lipid, and protein oxidation and excess nitric oxide/protein kinase G signaling in the ascending aorta. Consistent with preventing pathologic changes, cobinamide diminished aortic root dilation without affecting blood pressure. Cobinamide exhibited excellent safety and pharmacokinetic profiles indicating it could be a practical treatment. We conclude that cobinamide deserves further study as a disease-modifying treatment of Marfan Syndrome. (J Am Coll Cardiol Basic Trans Science 2024;9:46-62)

ABBREVIATIONS AND ACRONYMS

cGMP = cyclic guanosine monophosphate

H_2O_2 = hydrogen peroxide

JNK = c-Jun N-terminal kinase

MFS = Marfan Syndrome

MMP = matrix metalloproteinase

mRNA = messenger RNA

NO = nitric oxide

NOX = NADPH oxidase

NOS2 = inducible nitric oxide synthase

ONOO- = peroxynitrite

$O_2\cdot^-$ = superoxide

PBS = phosphate-buffered saline

PCR = polymerase chain reaction

PKG = protein kinase G

TAAD = thoracic aortic aneurysms and dissections

TGF = transforming growth factor

VASP = vasodilator-stimulated phosphoprotein

VSMC = vascular smooth muscle cell

Marfan Syndrome (MFS) is an autosomal-dominant disorder with a prevalence of ~1 in 5,000 people characterized by eye, skeletal, and cardiovascular abnormalities.[1,2] Aneurysm formation in the ascending aorta is the most serious manifestation and can lead to spontaneous aortic rupture and sudden death.[1,2] Current treatments of patients with MFS focus on reducing aortic wall stress using β-adrenergic and angiotensin receptor blockers; however, these agents are only partly effective and do not eliminate the need for aortic surgery.[3-8] Additional treatment options that address the underlying pathophysiology are needed.

The aorta derives its strength from a medial layer consisting of concentric layers of vascular smooth muscle cells (VSMCs) and elastin lamellae interspersed with collagen fibers. "Aortic media degeneration," defined by elastic fiber fragmentation, collagen and proteoglycan accumulation, and VSMC apoptosis, is a hallmark of MFS and other diseases with familial thoracic aortic aneurysms and dissection (TAAD), such as Ehlers-Danlos and Loeys-Dietz syndromes.[8-11]

MFS is due to deletions or loss-of-function mutations in fibrillin-1, an extracellular matrix protein that surrounds the elastin core of elastic fibers in the aortic media.[9,12] Fibrillin-1 has 96% amino acid sequence identity between mice and humans, consistent with mouse models of MFS recapitulating the human disease.[13] Mice heterozygous for a fibrillin-1 mutation ($Fbn1^{C1041G/+}$) analogous to a common mutation in patients with MFS develop aortic media degeneration and age-dependent aortic dilation.[13,14] In addition to providing structural integrity and compliance to the aortic wall, fibrillin-1 regulates cell-matrix interactions via integrins and modulates transforming growth factor (TGF)-β release from a latent complex.[9] Decreased connectivity between mutant fibrillin-1 and integrins[15] and increased bioactive TGF-β in the aortic media initiate phenotypic changes in VSMCs that result in aberrant gene expression.[16-18] TGF-β signals via canonical (Smad2/3) and noncanonical (ERK1/2, Jun-N-terminal kinase, and p38) pathways; increased noncanonical signaling promotes maladaptive aortic remodeling in adults, including induction of matrix metalloproteinases (MMPs) that contribute to elastic fiber fragmentation.[14,16,17,19-21]

In the aorta and VSMCs of patients with MFS and in Marfan mouse models, increased expression of inducible nitric oxide synthase (NOS2) and nicotinamide adenine dinucleotide phosphate (NADPH) oxidase 4 (NOX4) leads to increased production, respectively, of nitric oxide (·NO) and hydrogen peroxide (H_2O_2)/superoxide ($O_2\cdot^-$).[22-30] ·NO reacts with $O_2\cdot^-$ at a diffusion-limited rate to yield peroxynitrite (ONOO-), a potent nitrating agent.[31]

The authors attest they are in compliance with human studies committees and animal welfare regulations of the authors' institutions and Food and Drug Administration guidelines, including patient consent where appropriate. For more information, visit the Author Center.

Manuscript received February 13, 2023; revised manuscript received July 18, 2023, accepted July 24, 2023.

JACC: BASIC TO TRANSLATIONAL SCIENCE VOL. 9, NO. 1, 2024
JANUARY 2024:46–62

These highly reactive species can cause DNA, lipid, and protein oxidation and protein nitration, contributing to the aortic disease.[22-30]

Increased ·NO production can also activate guanylate cyclase and thereby protein kinase G (PKG), with increased ·NO/PKG signaling additionally contributing to aneurysm development in MFS.[24,32] Moreover, in a large study of patients with MFS, PKG1 was identified as 1 of 3 major loci determining severity of aortic disease, and a gain-of-function mutation in PKG1 leads to TAAD in humans.[33,34] In mice with an analogous PKG1 mutation (*Prkg1*$^{R177Q/+}$), we found age-dependent aortic dilation with media degeneration and increased expression of NOX4 and oxidative stress markers.[35]

The cobalamin (vitamin B_{12}) analog cobinamide is a powerful antioxidant, serving as both a superoxide dismutase and catalase mimetic, thereby neutralizing $O_2{\cdot}^-$ and H_2O_2, respectively[36] (cobinamide structure is shown in Supplemental Figure 1). In addition, cobinamide reacts with ·NO and ONOO-.[36,37] We, therefore, hypothesized that cobinamide could be an effective treatment for MFS, and tested it in *Fbn1*$^{C1041G/+}$ mutant male and female mice, assessing histopathology, oxidative stress markers, PKG activity, and aortic size.

METHODS

MATERIALS. Hydroxo-cobalamin, L-histidine, and cerium chloride were from Sigma-Aldrich. H_2O_2 was from Fisher Scientific, ONOO- was from Caymen Chemical, and 8-(4-chlorophenylthio) cyclic guanosine monophosphate (cGMP) (8-CPT-cGMP, a membrane-permeable cGMP analog) was from Biolog. An 8-isoprostane (8-*iso*-prostaglandin $F_{2\alpha}$) enzyme-linked immunosorbent assay system was from Cayman Chemical. An Apo-Tag Peroxidase In Situ Apoptosis Detection Kit was from Millipore-Sigma. Antibodies are listed in Supplemental Table 1.

Cobinamide was synthesized from cobalamin by base hydrolysis using freshly made cerium hydroxide (from cerium chloride) and was purified over 2 reversed-phase resin columns as described previously.[38] The resulting product was >98% pure as determined using high-performance liquid chromatography with ultraviolet detection, and using mass spectrometry. In aqueous solutions at neutral pH, a water and hydroxyl group are coordinated to the cobalt, ie, it is aquohydroxo-cobinamide (R = H_2O and OH in Supplemental Figure 1A). We generated histidyl-cobinamide (cobinamide with 2 bound histidine molecules) by adding 3 molar equivalents of L-histidine to aquohydroxo-cobinamide and adjusting the pH to 7.0. We administered histidyl-cobinamide to mice because it is stable in aqueous solutions, allowing it to be used in drinking water. It is referred to as "cobinamide" throughout the text.

MOUSE GENOTYPES AND HOUSING. *Fbn1*$^{C1041G/+}$ male mice in a C57BL/6J background were obtained from Jackson Laboratories (catalog no. 012885). These mice harbor a p.Cys1041Gly mutation in fibrillin-1 representative for a class of human missense mutations causing MFS.[13] The mutant mice were bred with female wild-type C57BL/6J (Jackson, catalog no. 000664) mice to generate wild-type and heterozygous mutant littermates. The genotypes of pups were determined using polymerase chain reaction (PCR) from a distal tail clip using the following primers: 5'-CTC ATC ATT TTT GGC CAG TTG-3' and 5'-GCA CTT GAT GCA CAT TCA CA-3' (wild-type allele 164 base pair [bp], mutant allele 212 bp). Mice were housed 3-4 mice per cage in a temperature-controlled environment with a 12-h light/dark cycle and fed standard rodent chow with ad libitum access to food and water.

COBINAMIDE TREATMENT. Shortly after weaning, ie, at about 4 weeks of age, cages containing wild-type and heterozygous littermates of each sex were assigned randomly to either plain drinking water or water containing 1 mmol/L cobinamide. The cobinamide-containing water was replenished twice weekly by filtering the water and filling the bottles. After 4 weeks, the solution was discarded, and fresh cobinamide-containing water was provided. The mice received cobinamide for 7 months, at which time their aortas were evaluated using ultrasonography, and they were euthanized. We chose 7 months of cobinamide treatment because 3 months of treatment showed a trend toward reduced aortic dilation that did not reach significance.

HARVESTING AORTAS. Mice were placed under deep anesthesia with 200 mg/kg ketamine and 40 mg/kg xylazine administered by intraperitoneal injection. The thoracic and peritoneal cavities were opened, the mice were exsanguinated via cardiac puncture, and the aorta was perfused in situ with ice-cold phosphate-buffered saline (PBS). The aorta was removed en-bloc with the heart and dissected from just above the aortic valve to the level of the diaphragm. The ascending aorta was fixed in 4% formaldehyde and the arch and descending aorta were flash frozen in liquid nitrogen. Paraffin-embedded blocks were made from the formaldehyde-fixed samples with the aortic segments cut transversely into 5 μm-thick sections that were mounted on glass slides.

HISTOLOGIC ANALYSES INCLUDING ASSESSMENT OF VSMC APOPTOSIS. Slides containing the mounted aortic sections were stained with hematoxylin-eosin (to count VSMC nuclei), Van Gieson's elastin stain (to detect elastin fiber breaks), and Mallory's trichrome stain (to quantify collagen, which stains blue). VSMC nuclei and elastin fiber breaks were counted manually at 40x magnification on 5 nonoverlapping areas of the aortic media measuring 0.025 μm^2 each; collagen content in a whole aortic cross-section was measured using Image-Pro Premier software (Version 9.0, Media Cybernetics) as described.[35] VSMC apoptosis was assessed using Tunel staining using the Apo-Tag Peroxidase In Situ Apoptosis Detection Kit per the manufacturer's instructions.[35] Briefly, slides were incubated in 10 mmol/L sodium citrate buffer, pH 6.0, and endogenous peroxidase activity was quenched in 3% H_2O_2. The 3'OH-DNA strand was labelled with digoxigenin-tagged nucleotides using terminal deoxynucleotidyl transferase. The slides were probed with anti-digoxigenin peroxidase antibody and developed with 3-diaminobenzidine (Vector Laboratories). Nuclei were counterstained with hematoxylin, and brown-stained nuclei were counted from 5 separate areas of the aortic media containing ~100 cells per area. All slides were scanned with a Hamamatsu Nanozoomer 2.0 HT scanning system and analyzed using Digital Pathology NDP.view2 software by an investigator who was blinded to the genotype and treatment of the mice.[35]

IMMUNOHISTOCHEMISTRY FOR 8-OH-DEOXYGUANOSINE, VASODILATOR-STIMULATED PHOSPHOPROTEIN PHOSPHORYLATION, PROTEIN NITRATION, AND MACROPHAGE PRESENCE. Slides with cross-sections of ascending aortas were incubated for 10 minutes in 10 mmol/L sodium citrate buffer, pH 6.0 at 80°C-85°C. Endogenous peroxidase activity was quenched in 3% H_2O_2 for 10 minutes. After blocking with 2% normal goat serum, slides were incubated overnight at 4°C with an anti-8-OH-deoxyguanosine, anti-nitrotyrosine, anti-phospho-vasodilator-stimulated phosphoprotein (VASP) Ser239, or anti-CD68 primary antibody, followed by a horseradish peroxidase-conjugated secondary antibody. After development with 3-diaminobenzidine (Vector Laboratories),[35] the samples were counterstained with hematoxylin, and images were scanned and analyzed as described above for histology. The number of brown-stained cells were counted from 5 separate areas of ~100 cells per area. Specificity of the anti-8-OH-deoxyguanosine, anti-nitrotyrosine, and anti-phospho-VASP Ser239 antibodies was shown by incubating freshly dissected aortas from wild-type mice, respectively, with 500 μmol/L H_2O_2 for 4 hours, 1 mmol/L ONOO- for 15 minutes, and 100 μmol/L 8-CPT-cGMP for 30 minutes at 37°C. In all cases, the aortas were in PBS. After the incubation, the aortas were fixed and processed as described earlier in this article. We found strongly positive staining of multiple VSMCs only in aortas incubated with the chemicals, but not in those incubated with PBS alone (Supplemental Figures 2A to 2C). We demonstrated specificity of the anti-CD68 antibody by staining mouse bone marrow with the antibody (Supplemental Figure 3).

WESTERN BLOTTING FOR PROTEIN CARBONYLATION AND P38 PHOSPHORYLATION. Protein carbonylation was assessed using the Oxyblot protein oxidation system from EMD Millipore. Frozen tissue was pulverized in liquid nitrogen and extracted in RIPA buffer containing 50 mmol/L dithiothreitol and protease inhibitors, with half of the extract (~5 μg protein) incubated with 2,4-dinitrophenylhydrazine. The samples were subjected to polyacrylamide gel electrophoresis immunoblotting, with carbonylated proteins detected using an anti-2,4-dinitrophenylhydrazine antibody.

To determine phosphorylation of p38 mitogen-activated protein kinase, frozen pieces of aorta (1-2 mg) were pulverized in liquid nitrogen, directly extracted in a sodium dodecyl sulfate-containing buffer, and heated to 100°C for 2 minutes. Western blots were developed with an anti-phospho-p38 (T180/Y182) antibody.

For both protein carbonylation and p38 phosphorylation, the blots were stripped and reprobed with an anti-β-actin antibody. Proteins were detected using chemiluminescence; band intensity was determined using densitometry on a LiCor Odyssey instrument and was normalized to actin.

ASSESSMENT OF 8-ISOPROSTANE CONTENT. 8-Isoprostanes were measured using enzyme-linked immunosorbent assay using frozen pieces of aorta (5-10 mg) pulverized in liquid nitrogen and processed according to the manufacturer's recommendation (Cayman Chemical). Each sample was measured in duplicate at 2 different dilutions; standard curves were included in each assay, and the data are expressed as picogram per milligram of wet tissue.

QUANTITATIVE REVERSE TRANSCRIPTION-PCR. Flash-frozen aortic tissue was pulverized and immersed in Trizol (Molecular Research Center, TR118). Total RNA was isolated, reverse-transcribed using iScript cDNA synthesis kit (Bio-Rad), and PCR was performed using a MX3005P real-time PCR

detection system with Brilliant II SYBR Green Mix (Agilent Technologies) as described.[35] Primer sequences are in Supplemental Table 2. All primers were intron-spanning (except for 18S ribosomal RNA), and were tested with serial complementary DNA dilutions. Relative changes in messenger RNA (mRNA) expression were analyzed using the comparative $2^{-\Delta\Delta Ct}$ method, with 18S ribosomal RNA serving as internal control.[35]

AORTIC ULTRASONOGRAPHY. One or two days before examination, a depilatory cream was applied to the anterior chest wall to remove hair. On the day of examination, mice were anesthetized with 5% isoflurane for 15 seconds and then maintained at 0.5% isoflurane throughout the examination. Small needle electrodes for a simultaneous electrocardiogram were inserted into 1 upper and 1 lower limb. Transthoracic ultrasonography was performed using the FUJIFILM VisualSonics Inc, Vevo 2100 high-resolution ultrasound system with a linear transducer of 32-55 MHz. Aortic dimensions were recorded during end-diastole at the aortic root by a single, highly experienced operator, who was blinded to genotype and treatment of the mice.[35]

MEASUREMENT OF BLOOD PRESSURE. The systolic and diastolic blood pressures of nonanesthetized mice were measured on the tail artery using the CODA Non-invasive Blood Pressure System (Kent Scientific) according to the manufacturer's recommendation. Recordings were obtained in a quiet room by a single operator after habituating the mice to the procedure for 5 days. Reported values are from 3 separate days over a 1-month period before euthanasia; on each day, 3 consecutive readings were obtained. Thus, for each mouse, the reported value represents the mean of 9 readings.

MEASUREMENT OF SERUM COBINAMIDE AND HISTIDINE CONCENTRATION. Whole blood from mice or rats was allowed to clot at room temperature and then was centrifuged at 5,000*g* for 5 minutes to remove cells. Serum concentrations of cobinamide and histidine were measured using high-performance liquid chromatography coupled with either mass spectrometry for cobinamide (Analytical and Diagnostic Solutions[39]) or ninhydrin post-column derivatization for histidine. The cobinamide and histidine were quantified by comparison to known standards.

PHARMACOKINETIC STUDIES. Sprague-Dawley rats weighing between 250 and 300 g were administered 80 mg/kg histidyl-cobinamide by oral gavage. Before drug administration and at 5, 15, and 30 minutes and 1, 2, 4, 8, and 24 hours after drug administration, blood was obtained from the external jugular vein. The studies were conducted at Attentive Science, LLC, Stilwell, KS. Cobinamide was measured in the serum as described earlier in this article.

POWER ANALYSIS AND STATISTICAL TESTS. Our primary hypothesis was that cobinamide would reduce the aortic dilation and pathologic changes that occur in *Fbn1*$^{C1041G/+}$ mice, without regard to sex. Based on a pilot study, we calculated that 12 animals per group would be sufficient to observe a 50% reduction in the aortic root dilation found in 8-month-old *Fbn1*$^{C1041G/+}$ mice compared with age-matched wild-type mice: 1.42 ± 0.26 mm for aortic root diameter of wild-type mice vs 1.98 ± 0.32 mm for mutant mice (mean ± SD; alpha error set at 0.05 and power set at 0.8). After randomization, the actual number of mice per group was: 15 untreated wild-type mice (8 males and 7 females); 13 treated wild-type mice (7 males and 6 females); 14 untreated *Fbn1*$^{C1041G/+}$ mice (8 males and 6 females); and 14 treated *Fbn1*$^{C1041G/+}$ mice (5 males and 9 females). All mice underwent ultrasonography for evaluation of aortic size, but, due to insufficient aortic tissue, not all aortas were subjected to the full suite of biochemical, histologic, and molecular analyses. In these cases, samples were selected randomly for each analysis, including samples from both males and females. Although the study was not powered to analyze males and females separately, we did perform subanalyses by sex when results were available for at least 5 mice in each group. Because we were interested only in whether cobinamide had an effect in both males and females, and not whether there was a differential effect between the 2 sexes, we performed separate analyses on the males and females.

All data are presented as the mean ± SD and were tested for normality using the Shapiro-Wilk test and for equality of variances using an F test. Only data sets that passed both tests were analyzed using a standard 2-way analysis of variance; when significant interaction ($P < 0.05$) was demonstrated, paired comparisons were made using the Bonferroni multiple comparisons test. Data that exhibited normality but not equality of variances were analyzed using a Welch analysis of variance followed by a Dunnett's T3 multiple comparisons test. Data that did not exhibit normality were analyzed using the nonparametric Kuskal-Wallis test followed by a Dunn test of multiple comparisons. Outliers were detected according to the robust regression and outlier removal method. All tests were conducted in GraphPad Prism 9.5.1, except

the F test, which was conducted using Statskingdom online calculator. A P value <0.05 was considered statistically significant.

STUDY APPROVAL. All animal experiments were conducted according to the National Academies of Sciences, Engineering, and Medicine Institute for Laboratory Animal Research Guide to the Care and Use of Laboratory Animals. The mouse experiments were approved by the Institutional Animal Care and Use Committee at the University of California-San Diego Protocol #S10121, and the rat experiments were approved by the Attentive Science Institutional Animal Care and Use Committee, Protocol #3120-0021.

RESULTS

COBINAMIDE REDUCES ELASTIN BREAKS AND PREVENTS COLLAGEN DEPOSITION IN THE AORTAS OF *Fbn1*$^{C1041G/+}$ MICE. Elastin fiber abnormalities and increased collagen deposition within the wall of the proximal aorta are prominent features in patients with MFS and *Fbn1*$^{C1041G/+}$ mice.[15,40,41] We found about a 6-fold increase in the number of elastin fiber breaks and a 3-fold increase in collagen in the ascending aortas of 8-month-old *Fbn1*$^{C1041G/+}$ mice compared with their wild-type littermates (**Figures 1A, 1B, 1D, and 1E**). Although difficult to quantify, the elastin fibers were flatter and less wavy in the mutant mice compared with the wild-type mice, a well-described change in elastin architecture.[42] Male and female mice showed a similar degree of abnormalities in elastin fibers and collagen deposition (**Figures 1C and 1F**). Administering cobinamide in the drinking water largely prevented the elastin fiber degeneration and eliminated the collagen accumulation in the mutant mice, exhibiting a similar beneficial effect in both males and females (**Figures 1A to 1F**). Cobinamide had no effect on elastin fiber morphology or collagen deposition in wild-type mice (**Figures 1A to 1F**).

COBINAMIDE PREVENTS SMOOTH MUSCLE CELL APOPTOSIS IN THE AORTAS OF *Fbn1*$^{C1041G/+}$ MICE. A decrease in the number of aortic VSMCs with an increase in VSMC apoptosis are also characteristic of MFS.[43] We found about a 50% reduction in the number of aortic VSMCs and twice as many apoptotic VSMCs in the ascending aortas of *Fbn1*$^{C1041G/+}$ mice compared with their wild-type littermates (**Figures 2A, 2B, 2D, and 2E**). Males and females showed a similar reduction in smooth muscle cell number, but only in females did the increase in apoptotic cells reach significance (**Figures 2C and 2F**). Cobinamide maintained a normal number of VSMCs and prevented the increase in apoptosis in the mutant mice (**Figures 2A, 2B, 2D, and 2E**), and reduced apoptosis in both sexes (**Figures 2C and 2F**).

COBINAMIDE REDUCES OXIDATIVE STRESS MARKERS IN THE AORTAS OF *Fbn1*$^{C1041G/+}$ MICE. Increased markers of oxidative stress have been shown in the aortas of patients with MFS and *Fbn1*$^{C1041G/+}$ mice.[22,23,29,44] We found almost a 3-fold increase in 8-OH-deoxyguanosine staining in the ascending aortas of 8-month-old mutant mice compared with wild-type siblings, indicating increased DNA oxidation (**Figures 3A and 3B**). Male and female mice showed a similar increase in 8-OH-deoxyguanosine staining (**Figure 3C**). Cobinamide prevented the increase in 8-OH-deoxyguanosine staining in the mutant mice (**Figure 3B**), and in both males and females (**Figure 3C**).

We found about a 4-fold increase in protein carbonylation and a 2-fold increase in 8-isoprostane content in the aortas of mutant mice compared with their wild-type littermates (**Figures 3D to 3F**). The former is a marker of protein oxidation and the latter is a marker of lipid oxidation. We had an insufficient amount of aortic tissue to analyze males and females separately. Cobinamide prevented the increase in protein and lipid oxidation in the mutant mice (**Figures 3D to 3F**).

Activation of p38 mitogen-activated protein kinase occurs as part of noncanonical TGF-β signaling and plays an important role in regulating VSMC apoptosis.[21,45] We found more than a 2-fold increase in p38 phosphorylation, ie, activation, in aortas of mutant mice compared with wild-type littermates, with cobinamide returning p38 phosphorylation to values found in wild-type mice (**Figures 3G and 3H**). The reduced p38 activation in cobinamide-treated animals is consistent with cobinamide's effect on reducing VSMC apoptosis (**Figures 2D to 2F**).

COBINAMIDE NORMALIZES EXPRESSION OF TGF-β- AND REDOX-RELATED GENES IN THE AORTAS OF *Fbn1*$^{C1041G/+}$ MICE. In accordance with previous studies, we found increased expression of *Tgfb1* (encoding *TGF-β1)* and its target genes *Serpine1*, *Col3a1*, and *Mmp2* in aortas of *Fbn1*$^{C1041G/+}$ mice compared with their wild-type littermates (**Figure 4A**).[16,46] Cobinamide reduced the expression of all 4 genes significantly, almost to values found in wild-type mice (**Figure 4A**). Expression of the housekeeping gene *Hprt* was similar in wild-type and mutant aortas, and was unaffected by cobinamide (**Figure 4A**). We also found increased expression of the pro-oxidant genes *Nox2* and *Nox4*, and decreased expression of the antioxidant gene *Sod2* in the mutant mice compared with their wild-type counterparts (**Figure 4B**), consistent with

FIGURE 1 Cbi Reduces Elastin Breaks and Prevents Collagen Deposition in the Aortas of *Fbn1*$^{C1041G/+}$ Mice

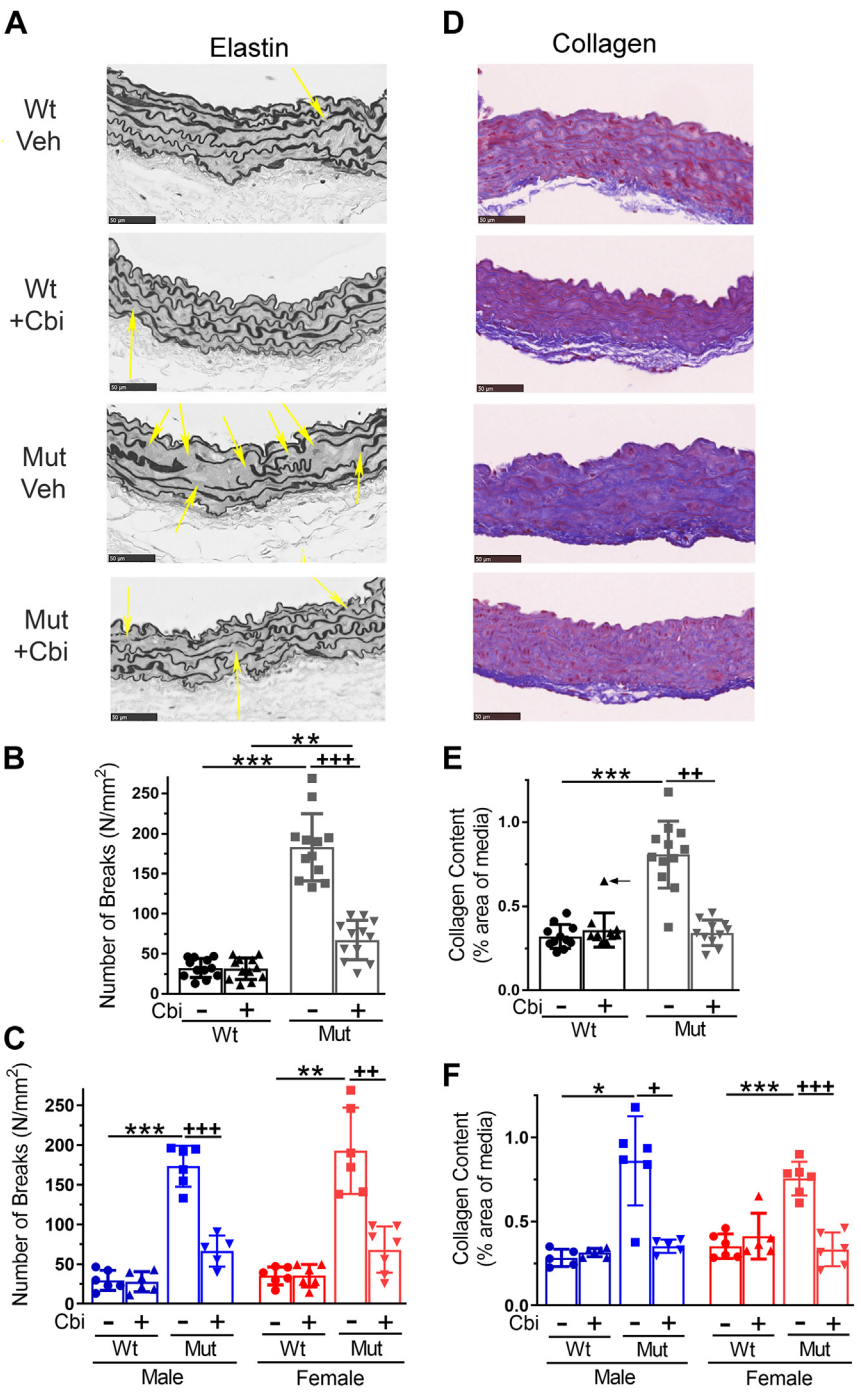

Wt and *Fbn1*$^{C1041G/+}$ mice were randomized to receive either 1 mmol/L histidyl-Cbi in their drinking water or plain water starting at 1 month of age until 8 months of age. The mice were then euthanized, and the ascending aorta was removed and fixed and sectioned for histologic analyses. (A to C) Slides were stained with Van Gieson's elastin stain, and elastin fiber breaks were counted in multiple, nonoverlapping fields as described in Methods. (D to F) Slides were stained with Mallory's trichrome stain, and the collagen content of the media was determined as the percentage of blue area in whole aortic cross-sections using Image-Pro Premier software. In all panels, slides were evaluated by an observer blinded to the genotype and treatment of the mice. (A) The yellow arrows point to elastin fiber breaks. (B, C, E, and F) Each symbol represents data from an individual mouse. (A and D) Scale bars are 50 μm. (E) Arrow denotes an outlier. (B, C, E, and F) Data are presented as mean ± SD. (B, C, and F) The data were analyzed using a Welch ANOVA, and (E) the data were analyzed using the nonparametric Kruskal-Wallis test. * or + $P < 0.05$; ** or ++ $P < 0.01$; *** or +++ $P < 0.001$, respectively, for the indicated comparisons; other group comparisons were not significantly different. ANOVA = analysis of variance; Cbi = cobinamide; Wt = wild type; Mut = *Fbn1*$^{C1041G/+}$ mutant.

FIGURE 2 **Cbi Prevents Smooth Muscle Cells Apoptosis in the Aortas of *Fbn1*$^{C1041G/+}$ Mice**

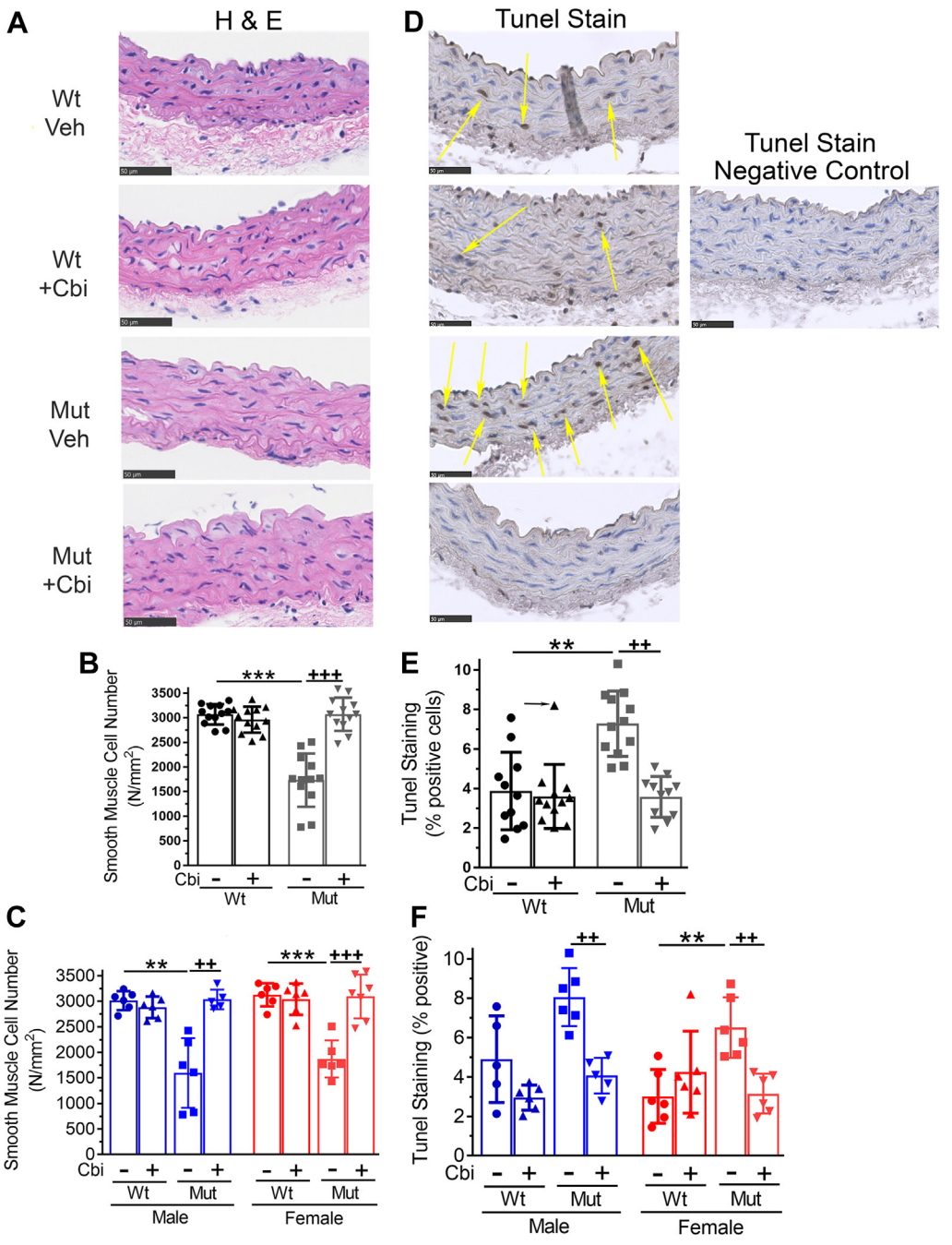

Wt and *Fbn1*$^{C1041G/+}$ mice were treated as described in Figure 1. At the time of euthanasia, the ascending aorta was fixed in formalin. (A to C) Slides were stained with hematoxylin-eosin and the number of smooth muscle cell nuclei were counted in multiple, nonoverlapping fields as described in Methods. (D to F) Slides were subjected to TUNEL staining as described in Methods; the percentage of apoptotic (brown) cells was determined from 5 separate areas of ~100 cells per area. In all panels, slides were evaluated by an observer blinded to the genotype and treatment of the mice. (D) Yellow arrows point to apoptotic smooth muscle cells. (B, C, E, and F) Each symbol represents data from an individual mouse. (A and D) Scale bars are 50 μm. (E) Arrow denotes an outlier. (B, C, E, and F) Data are presented as mean ± SD. (B, C, and F) The data were analyzed using a Welch ANOVA, and (E) the data were analyzed using the nonparametric Kruskal-Wallis test. ** or ++ $P < 0.01$, and *** or +++ $P < 0.001$, respectively, for the indicated comparisons; other group comparisons were not significantly different.
H&E = hematoxylin and eosin; other abbreviations as in Figure 1.

FIGURE 3 **Cbi Reduces Oxidative Stress Markers in the Aortas of *Fbn1*$^{C1041G/+}$ Mice**

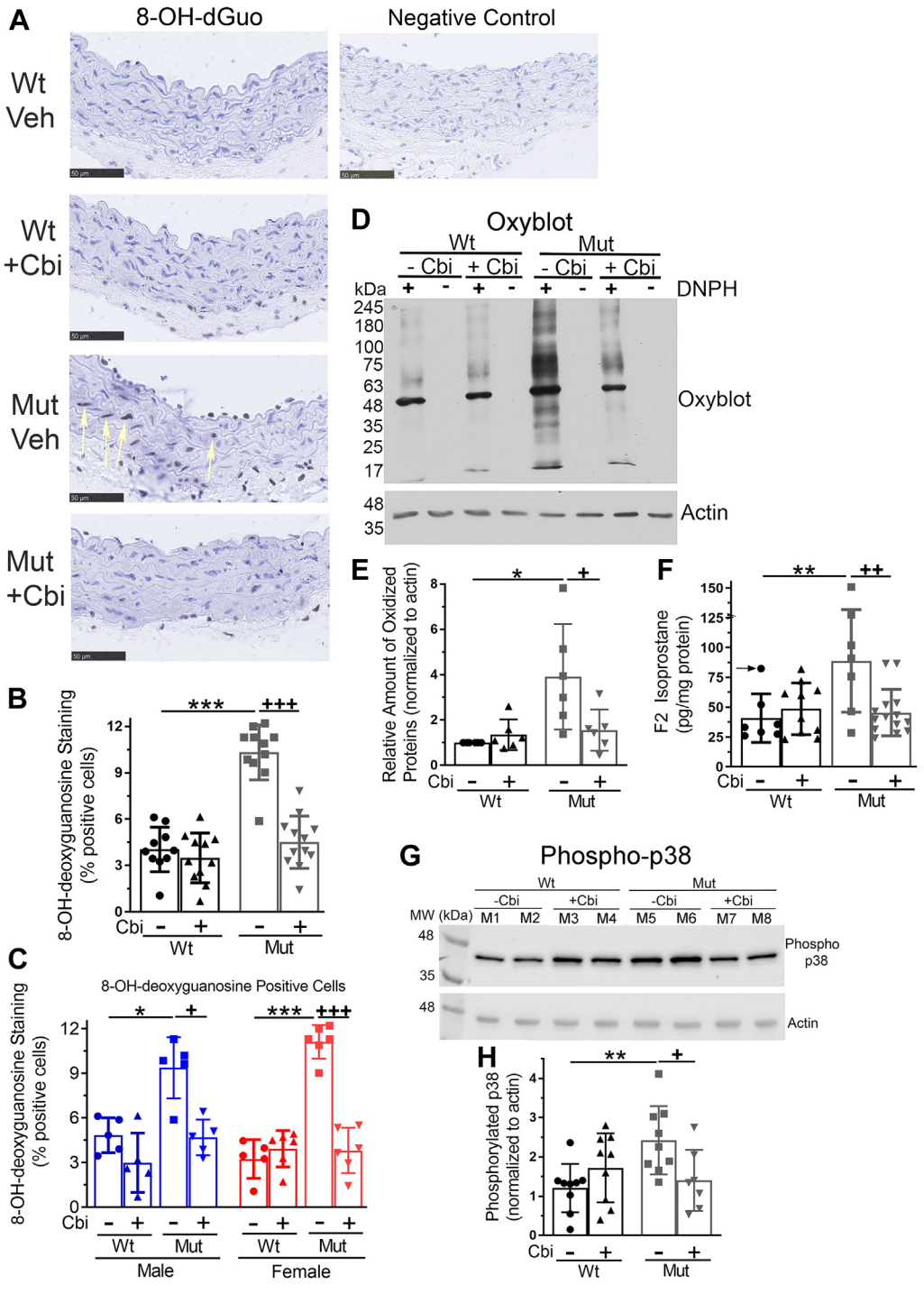

Continued on the next page

published reports.[23,24,44] Cobinamide markedly reduced expression of *Nox2* and *Nox4* and restored *Sod2* expression to values similar to those in wild-type mice (Figure 4B). Expression of PKG1 (gene name *Prkg1*) mRNA was similar in wild-type and mutant aortas, and was unaffected by cobinamide (Figure 4B).

COBINAMIDE REDUCES PROTEIN NITRATION AND PREVENTS EXCESS NO/cGMP/PKG PATHWAY ACTIVITY IN AORTAS OF *Fbn1*$^{C1041G/+}$ MICE. Increased ·NO production likely occurs in the aorta of patients with MFS and in *Fbn1*$^{C1041G/+}$ mice, based on increased NOS2 expression and protein nitration.[24,32] ·NO reacts with $O_2^{\cdot -}$ at a diffusion-limited rate to generate ONOO-; the latter dissociates into the nitrogen dioxide radical that can cause nitration of protein tyrosine residues.[31] We found about a 3-fold increase in protein nitrotyrosine content in the ascending aortas of *Fbn1*$^{C1041G/+}$ mice compared with their wild-type littermates, with cobinamide reducing the nitrotyrosine content almost back to the amount found in wild-type mice (Figures 5A and 5B).

A primary intracellular target of ·NO is soluble guanylate cyclase.[47] The resulting increase in cGMP activates PKG, and previous investigators have shown increased activation of the NO/cGMP/PKG pathway in the aortas of patients with MFS and *Fbn1*$^{C1041G/+}$ mice.[24,32] Consistent with these data, we found more than a 2-fold increase in phosphorylation of VASP on Ser^{239} in the ascending aorta of *Fbn1*$^{C1041G/+}$ mice compared with their wild-type littermates (Figures 5C and 5D); male and female mutant mice showed a similar increase in VASP Ser^{239} phosphorylation (Figure 5E). VASP phosphorylation on Ser^{239} is considered a specific marker of PKG activation.[48] Cobinamide prevented the excess Ser^{239} VASP phosphorylation in the mutant mice, and this occurred in both males and females (Figures 5C to 5E).

COBINAMIDE REDUCES DILATION OF THE PROXIMAL AORTA IN *Fbn1*$^{C1041G/+}$ MICE WITHOUT AFFECTING BLOOD PRESSURE. In patients with MFS and in *Fbn1*$^{C1041G/+}$ mice, aortic dilation affects primarily the aortic root.[2,16] We found a significant increase in the diameter of the aorta just above the aortic valve in the *Fbn1*$^{C1041G/+}$ mice compared with their wild-type littermates (Figure 6A). Cobinamide had no effect on aortic root size in wild-type mice, but reduced the diameter of the aortic root significantly in the mutant mice (Figure 6A). When males and females were analyzed separately, the mutant mice exhibited a similar increase in aortic root size in males and females compared with their wild-type littermates: to adjust for differences in body size between males and females, we normalized the aortic diameter to body weight and found a 0.021 mm/g and 0.018 mm/g increase in aortic size in males and females, respectively (Figure 6B). Cobinamide reduced the aortic diameter by a similar amount in both sexes (0.0091 mm/g vs 0.0088 mm/g in males and females, respectively), but only in males did the reduction reach significance (Figure 6B). The lack of a significant effect in the female mutant mice was due at least in part to greater variability in aortic measurements in the females than in the males (Figure 6B).

Cobinamide's effect on aortic dimensions was not due to a reduction in blood pressure, because cobinamide had no effect on blood pressure in either wild-type or mutant mice (Figure 6C shows mean arterial pressure for males and females combined, and Supplemental Figures 4A and 4B show systolic and diastolic blood pressures for males and females separately).

COBINAMIDE SERUM CONCENTRATION, SAFETY PROFILE, AND PHARMACOKINETICS. In mice that received cobinamide in their drinking water, the serum cobinamide concentration was 0.07 ± 0.02 and 0.08 ± 0.03 μmol/L in wild-type and *Fbn1*$^{C1041G/+}$

FIGURE 3 Continued

Wt and *Fbn1*$^{C1041G/+}$ mice were treated as described in Figure 1. At the time of euthanasia, the ascending aorta was fixed in formalin (A to C) and the remaining aortic arch was flash frozen in liquid nitrogen (D to H). (A to C) 8-OH-deoxyguanosine was assessed using immunohistochemistry using an anti-8-OH-deoxyguanosine antibody to determine DNA oxidation. Supplemental Figure 1A shows a positive control for the antibody. (D and E) Protein oxidation was assessed using the Oxyblot protein carbonylation detection system. Half of the extracts were incubated with 2,4-dinitrophenylhydrazine before gel electrophoresis. (F) 8-isoprostane was measured using ELISA to assess lipid oxidation. (G and H) Phosphorylated p38 was assessed using immunoblotting with an anti-p38 (pT180/pY182)-specific antibody. (A to C) Slides were evaluated by an observer blinded to the genotype and treatment of the mice. (A) The yellow arrows point to smooth muscle cells that stained with the anti-8-OH-deoxyguanosine antibody. (B, C, E, F, and H) Each symbol represents data from an individual mouse. (A) Scale bars are 50 μm. (F) Arrow denotes an outlier. (B, C, E, F, and H) Data are presented as mean ± SD. (B and H) The data were analyzed using a 2-way ANOVA, (C and E) the data were analyzed using a Welch ANOVA, and (F) the data were analyzed using the nonparametric Kruskal-Wallis test. * or + $P < 0.05$, ** or ++ $P < 0.01$, *** or +++ $P < 0.001$, respectively, for the indicated comparisons; other group comparisons were not significantly different. ELISA = enzyme-linked immunosorbent assay; M1-M8 = individual mice; phospho-p38 = phosphorylated p38; other abbreviations as in Figure 1.

JACC: BASIC TO TRANSLATIONAL SCIENCE VOL. 9, NO. 1, 2024
JANUARY 2024:46–62

FIGURE 4 Cbi Normalizes Expression of TGF-β- and Redox-Related Genes in the Aortas of *Fbn1*$^{C1041G/+}$ Mice

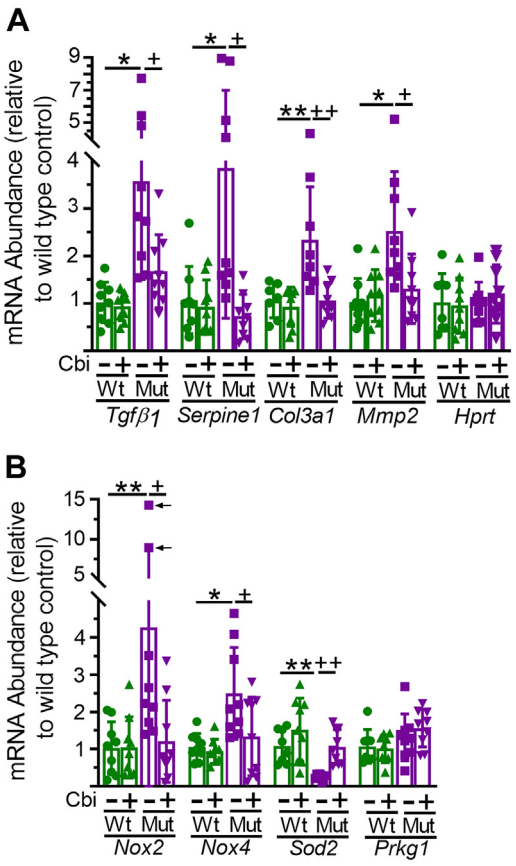

Wt and *Fbn1*$^{C1041G/+}$ mice were treated as described in Figure 1. At the time of euthanasia, the aortic arch was flash frozen in liquid nitrogen. (A and B) RNA was extracted and expression of the following genes was determined using RT-qPCR (the corresponding proteins are shown in parenthesis): *Tgfβ1* (TGF-β1), *Serpine1* (serine protease inhibitor-1, also known as plasminogen activator inhibitor-1), *Col3a1* (collagen 3α1), *MMP2* (matrix metalloproteinase-2), *Hprt* (hypoxanthine phosphoribosyl transferase), *Nox2* (NADPH oxidase-2), *Nox4* (NADPH oxidase-4), *Sod2* (superoxide dismutase-2), and *Prkg1* (protein kinase G-1). Data were normalized to 18S RNA and the mean ΔCt value obtained in untreated Wt mice was assigned a value of 1. Each symbol represents data from an individual mouse. (B) Arrows denote outliers. Data are presented as mean ± SD. (A) *Tgfβ1*, *Col3a1*, and *Mmp2* data were analyzed using a Welch ANOVA, and *Serpine1* data were analyzed using the nonparametric Kruskal-Wallis test. (B) *Nox4* and *Sod2* data were analyzed using a Welch ANOVA, and *Nox2* data were analyzed using the nonparametric Kruskal-Wallis test. * or + $P < 0.05$ and ** or ++ $P < 0.01$, respectively, for the indicated comparisons; other group comparisons were not significantly different. mRNA = messenger RNA; NADPH = nicotinamide adenine dinucleotide phosphate; RT-qPCR = reverse transcription-quantitative polymerase chain reaction; TGF = transforming growth factor; other abbreviations are as in Figure 1.

mice, respectively (mean ± SD from 4 mice per group, measured at the time of euthanasia between 9 AM and noon). Cobinamide was not measurable in the serum of mice that received plain drinking water. Serum histidine concentrations were not altered by the histidyl-cobinamide that was administered: serum histidine concentrations were 61 ± 11 μmol/L and 68 ± 9 μmol/L in mutant mice that received cobinamide and plain water, respectively (mean ± SD from 3 mice per group), similar to serum histidine concentrations in C57BL/6J mice.[49] Cobinamide treatment had no effect on water uptake, body weight, or standard clinical chemistry tests in both the wild-type and *Fbn1*$^{C1041G/+}$ mice (Figure 6D, Supplemental Tables 3 and 4). It had no effect on the complete blood count in wild-type mice but increased the percentage of monocytes from 2.5 ± 0.6 to 5.4 ± 1.3 in the *Fbn1*$^{C1041G/+}$ mice (Supplemental Table 3). The increase in monocytes was not accompanied by an increase in macrophage infiltration into the aorta (Supplemental Figure 3).

To assess the pharmacokinetics and half-life of cobinamide after oral administration, we administered the drug to rats using oral gavage; we used rats in these studies to allow for serial blood sampling. From these experiments, we estimate the half-life of cobinamide to be 11.3 h in rats (Supplemental Figure 4C).

DISCUSSION

Genetic and pharmacologic studies support a central role for increased oxidative and nitrosative stress in the pathogenesis of the aortic disease in MFS (Figure 7).[22,24,30,32] NOX4 and mitochondria are the likely sources of H_2O_2 and $O_2^{\cdot-}$ and NOS2 is the likely source of ·NO; $O_2^{\cdot-}$ reacts with ·NO to generate ONOO-.[22,24,29,30,32,50] The resultant protein oxidation and nitration can alter protein function.[51]

Increased ·NO can also activate PKG via guanylate cyclase and cGMP (Figure 7). Excessive PKG activation likely contributes to the pathophysiological changes in the Marfan aorta, because pharmacologic or genetic inhibition of NO/cGMP/PKG signaling reduces elastin fiber breaks and aortic dilation in Fbn1$^{C1041G/+}$ mice, and PKG1 expression modulates disease severity in patients with MFS.[24,32,33] PKG regulates VSMC differentiation, promoting a quiescent, hypercontractile phenotype, and it activates p38, ERK, and c-Jun N-terminal kinase (JNK) in aortic VSMCs.[35,52,53] Increased p38 kinase, ERK, and JNK activation in Marfan aortas and aortic VSMCs has been attributed to excessive noncanonical TGF-β signaling, but increased PKG activity likely

FIGURE 5 Cbi Reduces Protein Nitration and Prevents Excess NO/cGMP/PKG Pathway Activity in Aortas of *Fbn1*$^{C1041G/+}$ Mice

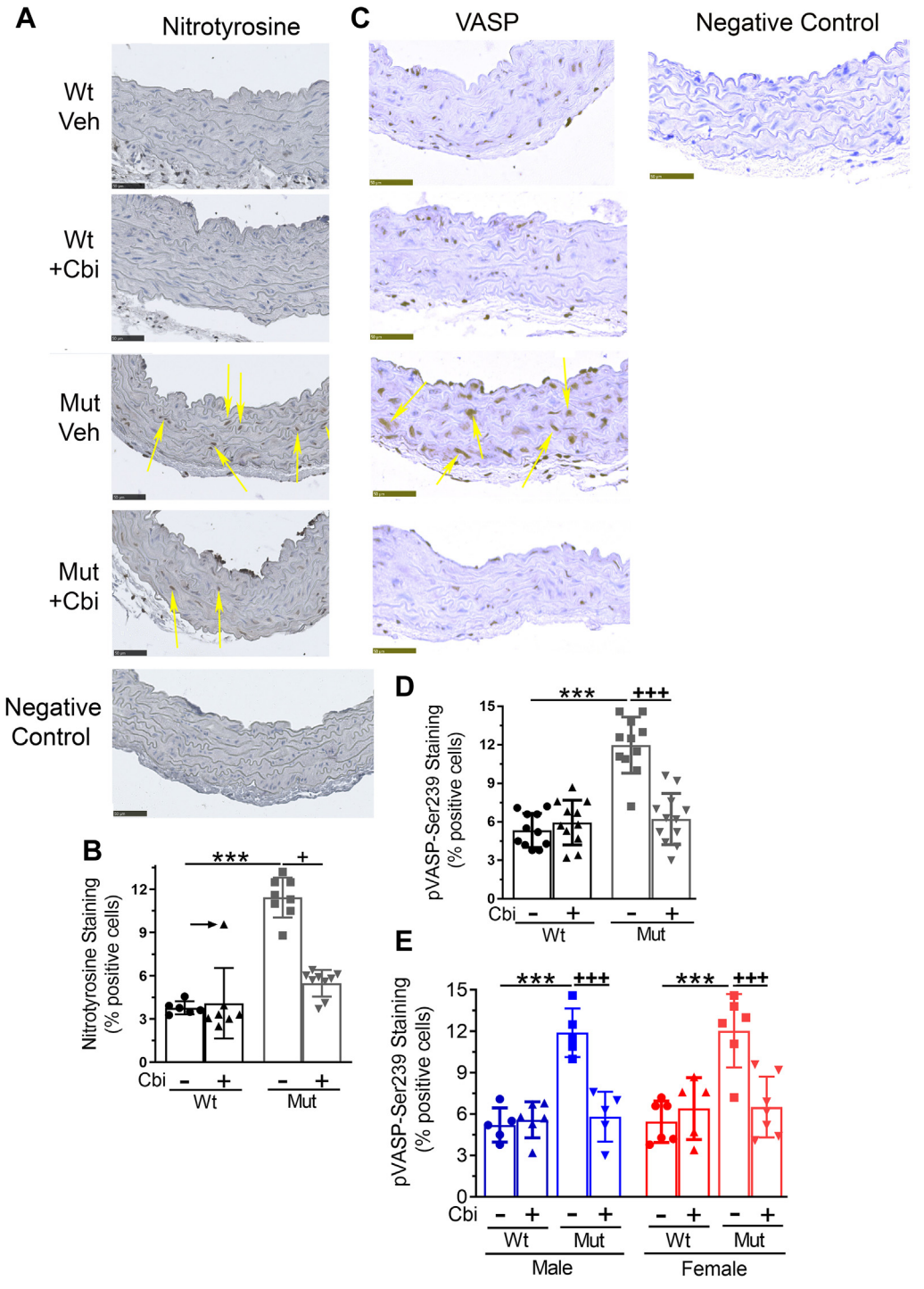

Continued on the next page

FIGURE 6 Cbi Reduces Dilation of the Proximal Aorta in *Fbn1*$^{C1041G/+}$ Mice Without Affecting Blood Pressure

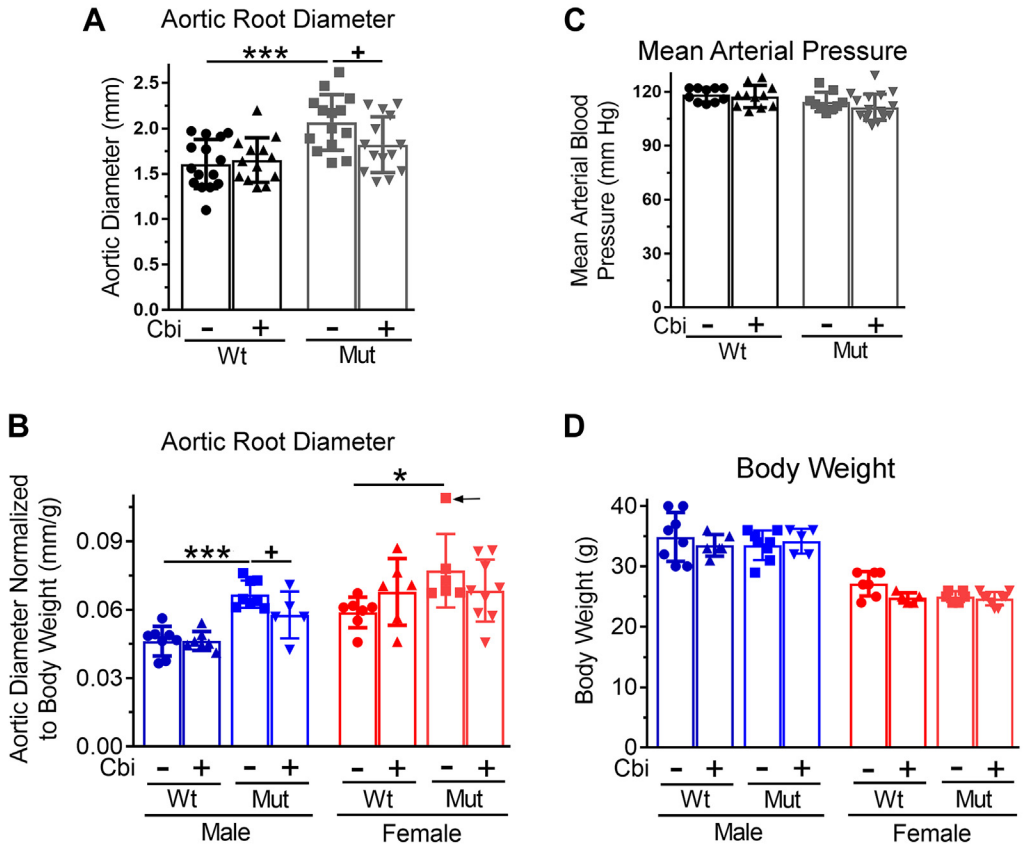

Wt and *Fbn1*$^{C1041G/+}$ mice were treated as described in the legend to Figure 1. During the month before euthanasia, their blood pressure was measured on 3 different occasions at least 1 week apart; their proximal aorta was visualized using ultrasonography 1-2 days before euthanasia. (A and B) The aortic root diameter was measured just above the aortic valve using ultrasonography in anesthetized mice. (B) For comparison between sexes, the aortic diameter was normalized to body weight. (C) The mean arterial blood pressure was measured using tail plethysmography in awake mice. (D) The mice were weighed on the day of ultrasonography. Each symbol represents data from an individual mouse. Data are presented as mean ± SD. (A and B) The data were analyzed using a 2-way ANOVA. * or + $P < 0.05$, ** $P < 0.01$, and ***$P < 0.001$, respectively, for the indicated comparisons; other group comparisons were not significantly different. (B) Arrow denotes an outlier. Abbreviations as in Figure 1.

FIGURE 5 Continued

Wt and *Fbn1*$^{C1041G/+}$ mice were treated as described in Figure 1. At the time of euthanasia, the ascending aorta was fixed in formalin. (A and B) Nitrotyrosine was assessed using immunohistochemistry. Supplemental Figure 1B shows a positive control for the antibody. (C-E) Phosphorylation of VASP Ser239 was assessed using immunohistochemistry. Supplemental Figure 1C shows a positive control for the antibody. In all panels, slides were evaluated by an observer blinded to the genotype and treatment of the mice. (A and C) The yellow arrows point to nitrotyrosine-positive and pVASP Ser239-positive cells, respectively. (A and C) Scale bars are 50 μm/L. (B) Arrow denotes an outlier. Each symbol represents data from an individual mouse. (B, D, and E) Data are presented as mean ± SD. (D and E) Data were analyzed using a 2-way ANOVA, and (B) data were analyzed using the nonparametric Kruskal-Wallis test. * or + $P < 0.05$, and *** or +++ $P < 0.001$, respectively, for the indicated comparisons; other group comparisons were not significantly different. cGMP = cyclic guanosine monophosphate; NO = nitric oxide; PKG = protein kinase G; VASP = vasodilator-stimulated phosphoprotein; abbreviations as in Figure 1.

contributes (Figure 7).[14,21,35,53] P38 activation leads to VSMC apoptosis, and JNK activation induces NOX4 and NOS2 expression, whereas ERK activation may increase expression of MMPs.[19,35,45,54,55] Reactive oxygen species may directly activate MMPs and promote VSMC apoptosis, with the activation of caspase-3 contributing to matrix proteolysis (Figure 7).[22,56] Altered VSMC mechanosensing and excess stretch in the Marfan aorta may further induce NOS2.[9,50,57] Several of these pathways constitute vicious cycles that likely augment oxidative and nitrosative stress in the Marfan aorta (Figure 7).

Because cobinamide is a strong antioxidant that can also modulate ·NO, we hypothesized it could be a potential treatment for MFS. We found that cobinamide dramatically reduced DNA, lipid, and protein oxidation, as well as protein nitration and VASP phosphorylation in the proximal aorta of *Fbn1*$^{C1041G/+}$ mice. Correspondingly, cobinamide prevented pathologic changes in the aorta and reduced aortic dilation. These data provide further evidence that oxidative and nitrosative stress and NO/cGMP/PKG signaling play a key role in the aortopathy in patients with MFS.

Cobinamide did not affect blood pressure in wild-type or mutant mice, indicating that its effect on NO/cGMP/PKG signaling was not sufficient to interfere with NO regulation of blood pressure, which requires activation of soluble guanylate cyclase and PKG in peripheral resistance blood vessels.[47] This is consistent with our previous results in mice treated with similar cobinamide concentrations in the drinking water.[36]

Several other agents with either antioxidant or NO-reducing properties have salutary effects in *Fbn1*$^{C1041G/+}$ mice: 1) apocynin, a plant-derived NOX inhibitor; 2) 1400W, a NOS2 inhibitor; 3) resveratrol, a polyphenol that scavenges reactive oxygen species; 4) nitro-oleic acid, a nitrated fatty acid that reduces NOS2 expression[22,24,41,58]; and 5) allopurinol, a xanthine oxidase inhibitor.[59] These agents reduced elastin fragmentation, but their effects on other pathologic changes such as smooth muscle cell number and apoptosis and collagen deposition were either not studied or yielded negative results. The antioxidant lipoic acid had no effect on elastin fiber breaks or aortic dilation in a different Marfan mouse model (mgΔ^{loxPneo} mice), although it reduced $O_2^{\cdot-}$.[40] This lack of a beneficial effect could be due to the more severe phenotype of mgΔ^{loxPneo} mice or because lipoic acid does not affect nitrosative stress and NO signaling; if the latter, then reducing oxidative stress alone may not be sufficient to prevent the pathologic changes in the Marfan aorta.

FIGURE 7 Aberrant Signaling Pathways and Cbi's Potential Mechanism(s) of Action in VSMCs in MFS

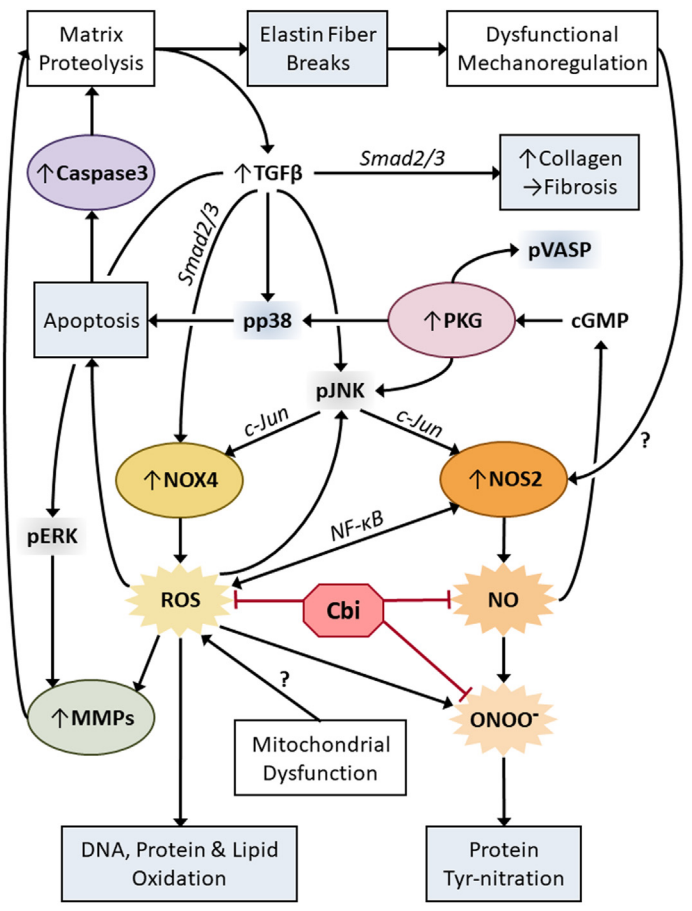

Enzymes are shown in ovals and processes are shown in rectangular boxes. MFS = Marfan Syndrome; MMPs = matrix metalloproteases; NOS2 = nitric oxide synthase 2; NOX4 = NADPH oxidase 4; ONOO- = peroxynitrite; pERK = phosphorylated extracellular signal-regulated kinase; pJNK = phosphorylated Jun N-terminal kinase; pp38 = phospho-p38; pVASP = phosphorylated VASP; ROS = reactive oxygen species; VSMCs = vascular smooth muscle cells; other abbreviations as in Figures 1, 4, and 5.

Although increased NO/cGMP/PKG signaling has been generally considered to have vaso-protective effects, excess PKG activity clearly can have detrimental effects in the cardiovascular system.[47,60] Phosphodiesterase-5 inhibitors, which activate PKG via inhibition of cGMP breakdown, aggravate the development of experimental abdominal aortic aneurysms in mice, and clinical case reports indicate an association between excessive use of phosphodiesterase-5 inhibitors and acute aortic

dissections.[61-64] Mice carrying the activating PKG1 mutation *Prkg1*$^{R177Q/+}$ develop aortic disease similar to that found in patients with familial TAAD carrying the same mutation; we showed that the increased PKG signaling in the aorta led to JNK-dependent NOX4 induction, increased oxidative stress, and dysregulated VSMC differentiation.[34,35] Cobinamide treatment completely prevented these changes as well as the associated age-related aortic dilation.[35] Thus, when combined with the current data, cobinamide has been effective in 2 different mouse models of human diseases where increased oxidative stress and aberrant PKG signaling are underlying causes of TAAD.

We found increased *Tgfb1*, *Serpine 1*, *Col3a1*, *Mmp2*, *Nox2*, and *Nox4* mRNA expression in the aortas of *Fbn1*$^{C1041G/+}$ mice, similar to gene expression changes reported previously in human and murine Marfan aortas and VSMCs.[50,65,66] Cobinamide almost completely prevented the increase in these gene transcripts, returning the mRNAs toward values found in wild-type mice. The affected genes are part of a "Marfan syndrome–specific gene signature" identified using transcriptomic profiling of human and murine Marfan aortas and indicate dysfunctional TGF-β signaling, which controls *Col3a1* and *Mmp2*.[65,66]

When evaluating *Fbn1*$^{C1041G/+}$ mice, most investigators have either not stated the gender, used males only, or reported combined data from males and females.[14,16,19,22-24,32,41,42,44,46,58] Two studies provided individual results on males and females and showed an increased number of elastin breaks in the aortas of males compared with females; one of the studies also reported greater aortic dilation in males than females.[44,67] Although our study was not powered to study sex-specific differences, we were able to do some subgroup analyses by sex and found similar increases in elastin fiber fragmentation and aortic root diameter in the 2 sexes. The difference between our results and the previous studies may be due to age: we used 8-month-old mice, whereas the previous studies used 3- to 6-month-old mice. Importantly, cobinamide reduced pathologic changes in both sexes; its effect on aortic size did not reach significance in the females, but this appeared due to greater variation in aortic size measurements in females than males.

The cobinamide-treated mice appeared normal and gained weight just as untreated mice, similar to our previous results in *Prkg1*$^{R177Q/+}$ mice and diabetic mice.[35,36] The only laboratory abnormality in the cobinamide-treated mice was an increase in peripheral blood monocytes, reaching significance in the mutant mice; the clinical implications of this are unclear, particularly because we found no increase in monocytic infiltration into the aorta. In rats, we found cobinamide had a serum half-life of ∼11 hours after oral administration. Rats generally clear drugs several times faster than humans, due in part to their higher basal metabolic rate, suggesting that cobinamide could be administered once daily to humans.[68,69] Thus, the safety and pharmacokinetic profiles of cobinamide indicate it could be a practical oral treatment for patients with MFS, but we should note that cobinamide has not yet been given to humans.

STUDY LIMITATIONS. First, we used *Fbn1*$^{C1041G/+}$ mice, which, in the absence of manipulation such as aortic constriction or angiotensin II infusion, have similar survival as wild-type mice until ∼12 months of age.[13,16] Thus, we were unable to determine if cobinamide improved survival of the mutant mice. Second, to minimize the number of animals used, we tested only one dose of cobinamide. Third, we cannot accurately calculate the cobinamide dose on a mg/kg basis, because we do not know the exact water volume consumed by each mouse; also, we do not know the bioavailability of cobinamide in mice, ie, how much of the ingested cobinamide was actually absorbed systemically. Fourth, we administered cobinamide as histidyl-cobinamide because it is more stable in solution than aquohydroxo-cobinamide. Histidine has some weak antioxidant properties,[70] but we found no increase in the plasma histidine concentration in mice that received cobinamide. And fifth, we did not test for reversal of cobinamide's near-complete resolution of the Marfan aortopathy; we would expect cobinamide's antioxidant effects to last only as long as the drug is administered, but restored elastic fiber integrity and improved media architecture could last beyond treatment termination.

CONCLUSIONS

The current drugs used in patients with MFS, β-adrenergic and angiotensin receptor-1 blockers, delay but do not completely prevent aortic dilation, singly or in combination.[3-8,11] Thus, a potentially disease-modifying treatment such as cobinamide that reduces aortic pathologic changes by controlling oxidative and nitrosative stress and restraining NO/cGMP/PKG signaling would be a welcome addition to the therapy for patients with MFS.

ACKNOWLEDGMENTS The authors acknowledge the University of California-San Diego Cardiovascular Laboratory, the University of California-San Diego

Microscopy Shared Facility supported by National Institutes of Health grant P30 NS047101, and Yusu Gu for expert execution of the ultrasonographic measurements.

FUNDING SUPPORT AND AUTHOR DISCLOSURES

The work was supported by National Institutes of Health grants U01 NS058030, U01 NS087964 to Dr Boss, and R01 HL132141 to Dr Pilz. Drs Kalyanaraman, Casteel, Boss, and Pilz are coinventors on a patent application entitled "New Treatment for Aortic Aneurysm." Dr Dretchen is the Chief Scientific Officer of Mesa Science Associates, a company that has interest in licensing cobinamide. All other authors have reported that they have no relationships relevant to the contents of this paper to disclose.

ADDRESS FOR CORRESPONDENCE: Dr Renate Pilz, Department of Medicine, University of California-San Diego, 9500 Gilman Drive, La Jolla, California 92093-0652, USA. E-mail: rpilz@ucsd.edu.

PERSPECTIVES

COMPETENCY IN MEDICAL KNOWLEDGE: In an established murine model of MFS, we confirm the impact of oxidative stress and excess nitric oxide production on aortic pathology. Mutant mice treated with the novel, potent antioxidant, and NO-quenching agent cobinamide show reduced aortic dilation, elastic fiber breaks, and smooth muscle cell apoptosis, and a reduction in multiple markers of oxidative and nitrosative stress in the aortic media.

TRANSLATIONAL OUTLOOK: The preclinical model strengthens the evidence for a causal role of oxidative and nitrosative stress in the development of aortic aneurysms in MFS. The unique antioxidant properties and favorable safety profile of cobinamide make it an excellent candidate for development as a novel disease-modifying treatment in MFS.

REFERENCES

1. Judge DP, Dietz HC. Marfan's syndrome. *Lancet*. 2005;366:1965–1976.

2. Keane MG, Pyeritz RE. Medical management of Marfan syndrome. *Circulation*. 2008;117:2802–2813.

3. Kocyigit D, Griffin BP, Xu B. Medical therapies for Marfan Syndrome and other thoracic aortic dilatation in adults: a contemporary review. *Am J Cardiovasc Drugs*. 2021;21:609–617.

4. Milewicz DM, Ramirez F. Therapies for thoracic aortic aneurysms and acute aortic dissections. *Arterioscler Thromb Vasc Biol*. 2019;39:126–136.

5. Singh MN, Lacro RV. Recent clinical drug trials evidence in Marfan Syndrome and clinical implications. *Can J Cardiol*. 2016;32:66–77.

6. Pitcher A, Spata E, Emberson J, et al. Marfan Treatment Trialists C. Angiotensin receptor blockers and beta blockers in Marfan syndrome: an individual patient data meta-analysis of randomised trials. *Lancet*. 2022;400:822–831.

7. Hofmann Bowman MA, Eagle KA, Milewicz DM. Update on clinical trials of losartan with and without beta-blockers to block aneurysm growth in patients with Marfan syndrome: a review. *JAMA Cardiol*. 2019;4:702–707.

8. Verstraeten A, Luyckx I, Loeys B. Aetiology and management of hereditary aortopathy. *Nat Rev Cardiol*. 2017;14:197–208.

9. Creamer TJ, Bramel EE, MacFarlane EG. Insights on the pathogenesis of aneurysm through the study of hereditary aortopathies. *Genes (Basel)*. 2021;12:183.

10. Shen YH, LeMaire SA, Webb NR, Cassis LA, Daugherty A, Lu HS. Aortic aneurysms and dissections series: Part II: dynamic signaling responses in aortic aneurysms and dissections. *Arterioscler Thromb Vasc Biol*. 2020;40:e78–e86.

11. Pyeritz RE. Etiology and pathogenesis of the Marfan syndrome: current understanding. *Ann Cardiothorac Surg*. 2017;6:595–598.

12. Ramirez F, Caescu C, Wondimu E, Galatioto J. Marfan syndrome; a connective tissue disease at the crossroads of mechanotransduction, TGFbeta signaling and cell stemness. *Matrix Biol*. 2018;71-72:82–89.

13. Judge DP, Biery NJ, Keene DR, et al. Evidence for a critical contribution of haploinsufficiency in the complex pathogenesis of Marfan syndrome. *J Clin Invest*. 2004;114:172–181.

14. Holm TM, Habashi JP, Doyle JJ, et al. Noncanonical TGFbeta signaling contributes to aortic aneurysm progression in Marfan syndrome mice. *Science*. 2011;332:358–361.

15. Bunton TE, Biery NJ, Myers L, Gayraud B, Ramirez F, Dietz HC. Phenotypic alteration of vascular smooth muscle cells precedes elastolysis in a mouse model of Marfan syndrome. *Circ Res*. 2001;88:37–43.

16. Habashi JP, Judge DP, Holm TM, et al. Losartan, an AT1 antagonist, prevents aortic aneurysm in a mouse model of Marfan syndrome. *Science*. 2006;312:117–121.

17. Cook JR, Clayton NP, Carta L, et al. Dimorphic effects of transforming growth factor-beta signaling during aortic aneurysm progression in mice suggest a combinatorial therapy for Marfan Syndrome. *Arterioscler Thromb Vasc Biol*. 2015;35:911–917.

18. Arce C, Rodriguez-Rovira I, De Rycke K, et al. Anti-TGFbeta (transforming growth factor beta) therapy with betaglycan-derived P144 peptide gene delivery prevents the formation of aortic aneurysm in a mouse model of Marfan Syndrome. *Arterioscler Thromb Vasc Biol*. 2021;41:e440–e452.

19. Habashi JP, Doyle JJ, Holm TM, et al. Angiotensin II type 2 receptor signaling attenuates aortic aneurysm in mice through ERK antagonism. *Science*. 2011;332:361–365.

20. Daugherty A, Chen Z, Sawada H, Rateri DL, Sheppard MB. Transforming growth factor-beta in thoracic aortic aneurysms: good, bad, or irrelevant? *J Am Heart Assoc*. 2017;6:e005221.

21. Carta L, Smaldone S, Zilberberg L, et al. p38 MAPK is an early determinant of promiscuous Smad2/3 signaling in the aortas of fibrillin-1 (*Fbn1*)-null mice. *J Biol Chem*. 2009;284:5630–5636.

22. Emrich F, Penov K, Arakawa M, et al. Anatomically specific reactive oxygen species production participates in Marfan syndrome aneurysm formation. *J Cell Mol Med*. 2019;23:7000–7009.

23. Yang HH, van BC, Chung AW. Vasomotor dysfunction in the thoracic aorta of Marfan syndrome is associated with accumulation of oxidative stress. *Vascul Pharmacol*. 2010;52:37–45.

24. Oller J, Mendez-Barbero N, Ruiz EJ, et al. Nitric oxide mediates aortic disease in mice deficient in the metalloprotease Adamts1 and in a mouse model of Marfan syndrome. *Nat Med*. 2017;23:200–212.

25. Huang K, Wang Y, Siu KL, Zhang Y, Cai H. Targeting feed-forward signaling of TGFbeta/NOX4/DHFR/eNOS uncoupling/TGFbeta axis with anti-TGFbeta and folic acid attenuates formation of aortic aneurysms: novel mechanisms and therapeutics. *Redox Biol*. 2021;38:101757.

26. Ejiri J, Inoue N, Tsukube T, et al. Oxidative stress in the pathogenesis of thoracic aortic aneurysm: protective role of statin and angiotensin II type 1 receptor blocker. *Cardiovasc Res*. 2003;59:988–996.

27. Fiorillo C, Becatti M, Attanasio M, et al. Evidence for oxidative stress in plasma of patients with Marfan syndrome. *Int J Cardiol*. 2010;145:544–546.

28. Soto ME, Soria-Castro E, Lans VG, et al. Analysis of oxidative stress enzymes and structural and functional proteins on human aortic tissue from different aortopathies. *Oxid Med Cell Longev*. 2014;2014:760694.

29. Portelli SS, Hambly BD, Jeremy RW, Robertson EN. Oxidative stress in genetically triggered thoracic aortic aneurysm: role in pathogenesis and therapeutic opportunities. *Redox Rep*. 2021;26:45–52.

30. Jimenez-Altayo F, Meirelles T, Crosas-Molist E, et al. Redox stress in Marfan syndrome: dissecting the role of the NADPH oxidase NOX4 in aortic aneurysm. *Free Radic Biol Med*. 2018;118:44–58.

31. Szabo C, Ischiropoulos H, Radi R. Peroxynitrite: biochemistry, pathophysiology and development of therapeutics. *Nat Rev Drug Discov*. 2007;6:662–680.

32. de la Fuente-Alonso A, Toral M, Alfayate A, et al. Aortic disease in Marfan syndrome is caused by overactivation of sGC-PRKG signaling by NO. *Nat Commun*. 2021;12:2628.

33. Aubart M, Gazal S, Arnaud P, et al. Association of modifiers and other genetic factors explain Marfan syndrome clinical variability. *Eur J Hum Genet*. 2018;26:1759–1772.

34. Guo DC, Regalado E, Casteel DE, et al. Recurrent gain-of-function mutation in PRKG1 causes thoracic aortic aneurysms and acute aortic dissections. *Am J Hum Genet*. 2013;93:398–404.

35. Schwaerzer GK, Kalyanaraman H, Casteel DE, et al. Aortic pathology from protein kinase G activation is prevented by an antioxidant vitamin B12 analog. *Nat Commun*. 2019;10:3533.

36. Chang S, Tat J, Pal China S, et al. Cobinamide is a strong and versatile antioxidant that overcomes oxidative stress in cells, flies, and diabetic mice. *PNAS Nexus*. 2022;1:1–13.

37. Sharma VS, Pilz RB, Boss GB, Magde D. Reactions of nitric oxide with vitamin B12 and its precursor, cobinamide. *Biochemistry*. 2003;42:8900–8908.

38. Chan A, Jiang J, Fridman A, et al. Nitrocobinamide, a new cyanide antidote that can be administered by intramuscular injection. *J Med Chem*. 2015;58:1750–1759.

39. Stutelberg MW, Dzisam JK, Monteil AR, et al. Simultaneous determination of 3-mercaptopyruvate and cobinamide in plasma by liquid chromatography-tandem mass spectrometry. *J Chromatogr B Analyt Technol Biomed Life Sci*. 2016;1008:181–188.

40. Guido MC, Debbas V, Salemi VM, et al. Effect of the antioxidant lipoic acid in aortic phenotype in a Marfan Syndrome mouse model. *Oxid Med Cell Longev*. 2018;2018:3967213.

41. Nettersheim FS, Lemties J, Braumann S, et al. Nitro-oleic acid reduces thoracic aortic aneurysm progression in a mouse model of Marfan syndrome. *Cardiovasc Res*. 2022;118:2211–2225.

42. Chung AW, Yang HH, Radomski MW, van Breemen C. Long-term doxycycline is more effective than atenolol to prevent thoracic aortic aneurysm in marfan syndrome through the inhibition of matrix metalloproteinase-2 and -9. *Circ Res*. 2008;102:e73–e85.

43. Quintana RA, Taylor WR. Cellular mechanisms of aortic aneurysm formation. *Circ Res*. 2019;124:607–618.

44. Jimenez-Altayo F, Siegert AM, Bonorino F, et al. Differences in the thoracic aorta by region and sex in a murine model of Marfan Syndrome. *Front Physiol*. 2017;8:933.

45. Granata A, Serrano F, Bernard WG, et al. An iPSC-derived vascular model of Marfan syndrome identifies key mediators of smooth muscle cell death. *Nat Genet*. 2017;49:97–109.

46. Chung AW, Au Yeung K, Sandor GG, Judge DP, Dietz HC, van Breemen C. Loss of elastic fiber integrity and reduction of vascular smooth muscle contraction resulting from the upregulated activities of matrix metalloproteinase-2 and -9 in the thoracic aortic aneurysm in Marfan syndrome. *Circ Res*. 2007;101:512–522.

47. Farah C, Michel LYM, Balligand JL. Nitric oxide signalling in cardiovascular health and disease. *Nat Rev Cardiol*. 2018;15:292–316.

48. Smolenski A, Bachmann C, Reinhard K, et al. Analysis and regulation of vasodilator-stimulated phosphoprotein serine 239 phosphorylation in vitro and in intact cells using a phosphospecific monoclonal antibody. *J Biol Chem*. 1998;273:20029–20035.

49. Takach E, O'Shea T, Liu H. High-throughput quantitation of amino acids in rat and mouse biological matrices using stable isotope labeling and UPLC-MS/MS analysis. *J Chromatogr B Analyt Technol Biomed Life Sci*. 2014;964:180–190.

50. Oller J, Gabande-Rodriguez E, Ruiz-Rodriguez MJ, et al. Extracellular tuning of mitochondrial respiration leads to aortic aneurysm. *Circulation*. 2021;143:2091–2109.

51. Xu Q, Huff LP, Fujii M, Griendling KK. Redox regulation of the actin cytoskeleton and its role in the vascular system. *Free Radic Biol Med*. 2017;109:84–107.

52. Zhang T, Zhuang S, Casteel DE, Looney DJ, Boss GR, Pilz RB. A cysteine-rich LIM-only protein mediates regulation of smooth muscle-specific gene expression by cGMP-dependent protein kinase. *J Biol Chem*. 2007;282:33367–33380.

53. Komalavilas P, Shah PK, Jo H, Lincoln TM. Activation of mitogen-activated protein kinase pathways by cyclic GMP and cyclic GMP-dependent protein kinase in contractile vascular smooth muscle cells. *J Biol Chem*. 1999;274:34301–34309.

54. Pawate S, Bhat NR. C-Jun N-terminal kinase (JNK) regulation of iNOS expression in glial cells: predominant role of JNK1 isoform. *Antioxid Redox Signal*. 2006;8:903–909.

55. Xiong W, Meisinger T, Knispel R, Worth JM, Baxter BT. MMP-2 regulates Erk1/2 phosphorylation and aortic dilatation in Marfan syndrome. *Circ Res*. 2012;110:e92–e101.

56. Emrich FC, Okamura H, Dalal AR, et al. Enhanced caspase activity contributes to aortic wall remodeling and early aneurysm development in a murine model of Marfan syndrome. *Arterioscler Thromb Vasc Biol*. 2015;35:146–154.

57. Zhao J, Nakahira K, Kimura A, Kyotani Y, Yoshizumi M. Upregulation of iNOS protects cyclic mechanical stretch-induced cell death in rat aorta smooth muscle cells. *Int J Mol Sci*. 2020;21:8660.

58. Hibender S, Franken R, van Roomen C, et al. Resveratrol inhibits aortic root dilatation in the Fbn1C1039G/+ Marfan mouse model. *Arterioscler Thromb Vasc Biol*. 2016;36:1618–1626.

59. Rodriguez-Rovira I, Arce C, De Rycke K, et al. Allopurinol blocks aortic aneurysm in a mouse model of Marfan syndrome via reducing aortic oxidative stress. *Free Radic Biol Med*. 2022;193:538–550.

60. Lundberg JO, Gladwin MT, Weitzberg E. Strategies to increase nitric oxide signalling in cardiovascular disease. *Nat Rev Drug Discov*. 2015;14:623–641.

61. Lameijer CM, Tielliu IF, van Driel MF, Zeebregts CJ. Type B aortic dissection after the use of tadalafil. *Ann Thorac Surg*. 2012;93:651–653.

62. Famularo G, Polchi S, Di BG, Manzara C. Acute aortic dissection after cocaine and sildenafil abuse. *J Emerg Med*. 2001;21:78–79.

63. Nachtnebel A, Stollberger C, Ehrlich M, Finsterer J. Aortic dissection after sildenafil-induced erection. *South Med J*. 2006;99:1151–1152.

64. Zhang C, Mohan A, Shi H, Yan C. Sildenafil (Viagra) aggravates the development of experimental abdominal aortic aneurysm. *J Am Heart Assoc*. 2022;11:e023053.

65. Dawson A, Li Y, Li Y, et al. Single-cell analysis of aneurysmal aortic tissue in patients with Marfan Syndrome reveals dysfunctional TGF-beta signaling. *Genes (Basel)*. 2021;13:95.

66. Pedroza AJ, Tashima Y, Shad R, et al. Single-cell transcriptomic profiling of vascular smooth muscle cell phenotype modulation in Marfan Syndrome aortic aneurysm. *Arterioscler Thromb Vasc Biol*. 2020;40:2195–2211.

67. Tashima Y, He H, Cui JZ, et al. Androgens accentuate TGF-beta dependent Erk/Smad activation during thoracic aortic aneurysm formation in Marfan Syndrome male mice. *J Am Heart Assoc*. 2020;9:e015773.

68. Nau H. Species differences in pharmacokinetics and drug teratogenesis. *Environ Health Perspect*. 1986;70:113–129.

69. Agoston DV. How to translate time? The temporal aspect of human and rodent biology. *Front Neurol*. 2017;8:92.

70. Wade AM, Tucker HN. Antioxidant characteristics of L-histidine. *J Nutr Biochem*. 1998;9:308–315.

KEY WORDS aortic aneurysm, *Fbn1*$^{C1041G/+}$ mutant mice, nitrosative stress, oxidative stress, protein kinase G

APPENDIX For supplemental figures and tables, please see the online version of this paper.